Catalytic Mechanism of Endonuclease V: A Catalytic and Regulatory Two-Metal Model†

Hong Feng, Liang Dong, and Weiguo Cao*

Department of Genetics and Biochemistry, South Carolina Experiment Station, Clemson University, Room 219, Biosystems Research Complex, 51 New Cherry Street, Clemson, South Carolina 29634

Received March 14, 2006; Revised Manuscript Received May 7, 2006

ABSTRACT: The enzyme endonuclease V initiates repair of deaminated DNA bases by making an endonucleolytic incision on the 3′ side one nucleotide from a base lesion. In this study, we have used site-directed mutagenesis to characterize the role of the highly conserved residues D43, E89, D110, and H214 in *Thermotoga maritima* endonuclease V catalysis. DNA cleavage and Mn^{2+}-rescue analysis suggest that amino acid substitutions at D43 impede the enzymatic activity severely while mutations at E89 and D110 may be tolerated. Mutations at H214 yield enzyme that maintains significant DNA cleavage activity. The H214D mutant exhibits little change in substrate specificity or DNA cleavage kinetics, suggesting the exchangeability between His and Asp at this site. DNA binding analysis implicates the involvement of the four residues in metal binding. Mn^{2+}-mediated cleavage of inosine-containing DNA is stimulated by the addition of Ca^{2+}, a metal ion that does not support catalysis. The effects of Mn^{2+} on Mg^{2+}-mediated DNA cleavage show a complexed initial stimulatory and later inhibitory pattern. The data obtained from the dual metal ion analyses lead to the notion that two metal ions are involved in endonuclease V-mediated catalysis. A catalytic and regulatory two-metal model is proposed.

Endonuclease V (endo V)[1] is a DNA repair enzyme which hydrolyzes the second phosphodiester bond 3′ from a deaminated base lesion. These lesions include inosine, xanthosine, oxanosine, and uridine (*1*−*5*). Endo V family proteins have been ubiquitously found in eubacteria, archaea, and eukaryotes including fission yeast, mice, and humans. Although the size of eukaryotic endo V homologues is larger than the prokaryotic counterparts, the amino acid residues essential for deaminated base recognition and DNA cleavage are well conserved (*6*). Using the thermostable endo V from *Thermotoga maritima* as a model system, we previously identified a series of amino acid residues that affect protein−DNA interactions (*6*). However, the active site architecture and metal ion coordination are not well understood.

Sequence alignment of the rapidly accumulating genomic data allowed us to identify seven conserved motifs in endo V family proteins (*6*). The highly conserved or invariant D43, E89, D110, and H214 are located in motifs II, III, IV, and VII, respectively (Figure 1). In this study, we probed these residues by constructing a series of site-directed mutants and conducting a comprehensive biochemical analysis. The mutability of the active site residues was determined using double-stranded and single-stranded inosine, xanthosine, oxanosine, and uridine DNA substrates. The binding affinities to inosine substrates were measured by gel mobility shift analysis in the absence and presence of metal cofactor. Since many endo V family proteins contain an Asp residue at a position equivalent to H214 in Tma endo V (Figure 1), cleavage kinetics was compared between the wild-type endo V and the H214D mutant. Effects of using alternative metal cofactor on inosine cleavage and 3′-exonuclease activity were assessed. Stimulation of Mn^{2+}-mediated inosine cleavage was observed, which led to a two-metal model for endonuclease V-mediated catalysis.

EXPERIMENTAL PROCEDURES

Reagents, Media, and Strains. All routine chemical reagents were purchased from Sigma Chemicals (St. Louis, MO), Fisher Scientific (Suwanee, GA), or VWR (Suwanee, GA). Restriction enzymes and T4 DNA ligase were purchased from New England Biolabs (Beverly, MA). DNA sequencing kits were purchased from Applied Biosystems (Foster City, CA). BSA and dNTPs were purchased from Promega (Madison, WI). *Taq* DNA polymerase was purchased from Eppendorf (Hamburg, Germany). Deoxyribooligonucleotides were ordered from Integrated DNA Technologies Inc. (Coralville, IA). LB medium was prepared according to standard recipes. Tma endo V sonication buffer consisted of 20 mM HEPES−KOH (pH 7.4), 1 mM EDTA (pH 8.0), 0.5 mM DTT, 0.1 mM PMSF, and 50 mM NaCl. GeneScan stop buffer consisted of 80% formamide (Amresco, Solon, OH), 50 mM EDTA (pH 8.0), and 1% blue dextran (Sigma Chemicals). TB buffer (1×) consisted of 89

† This work was supported in part by CSREES/USDA (SC-1700274, Technical Contribution No. 5093), the NIH (GM 067744), the Concern Foundation, and the DOD−Army Research Office (W911NF-05-1-0335).

* Corresponding author: e-mail, wgc@clemson.edu; tel, (864) 656-4176; fax, (864) 656-0393.

[1] Abbreviations: BSA, bovine serum albumin; dNTP, deoxyribonucleoside triphosphate; DTT, dithiothreitol; 6-Fam, 6-carboxyfluorescein; *E. coli*, *Escherichia coli*; endo V, endonuclease V; HEPES, *N*-(2-hydroxyethyl)piperazine-*N*′-2-ethanesulfonic acid; I, deoxyinosine; PAGE, polyacrylamide gel electrophoresis; PCR, polymerase chain reaction; PMSF, phenylmethanesulfonyl fluoride; Tma, *Thermotoga maritima*; wt, wild type.

10.1021/bi060512b CCC: $33.50
Published on Web 08/04/2006

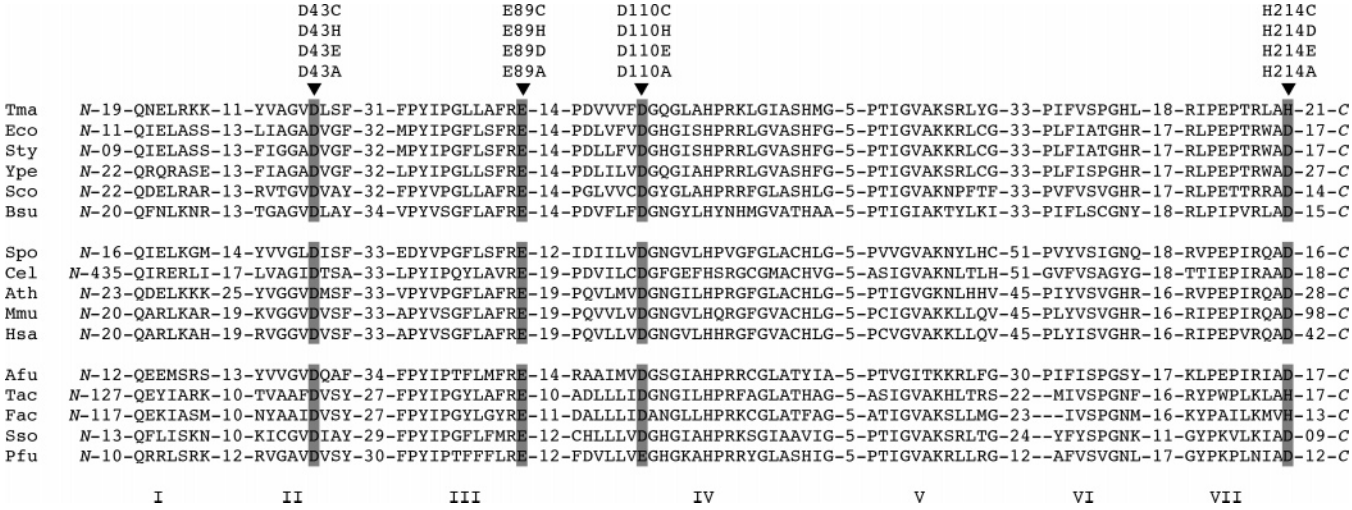

FIGURE 1: Sequence alignment of endonuclease V. Amino acid residues selected for site-directed mutagenesis are highlighted, and the resulting mutants are indicated above the arrows. GenBank accession numbers are shown after the species names. Key: Tma, *T. maritima*, NP_229661; Eco, *E. coli*, NP_418426; Sty, *Salmonella typhimurium*, NP_463037; Ype, *Yersinia pestis*, NP_667835; Sco, *Streptomyces coelicolor*, CAB40676; Bsu, *Bacillus subtilis*, BSUB0019; Spo, *Schizosaccharomyces pombe*, 1723511; Cel, *Caenorhabditis elegans*, 1731299; Ath, *Arabidopsis thaliana*, T10669; Mmu, *Mus musculus*, XP_203558; Hsa, *Homo sapiens*, BAC04765; Afu, *Archaeoglobus fulgidus*, NP_068968; Tac, *Thermoplasma acidophilum*, CAC11602; Fac, *Ferroplasma acidarmanus*, ZP_00001774; Sso, *Sulfolobus solfataricus*, NP_343804; Pfu, *P. furiosus*, NP_578716.

mM Tris base and 89 mM boric acid. TE buffer consisted of 10 mM Tris-HCl, pH 8.0, and 1 mM EDTA. *Escherichia coli* host strain AK53 (*mrr*B$^-$, MM294) was from our laboratory collection.

Site-Directed Mutagenesis of Tma Endo V. An overlapping extension PCR procedure was used for site-directed mutagenesis (*7*). Details of site-directed mutagenesis and protein purification and quantitation were essentially carried out as previously described (*8*).

Oligodeoxyribonucleotide Substrates. The sequences of the oligonucleotides were shown in Figure 2A. Oligonucleotides containing inosine or uridine were ordered from IDT, purified by PAGE, and dissolved in TE buffer at a final concentration of 10 μM. The two complementary strands (with the unlabeled strand in 1.2-fold molar excess) were mixed and incubated at 85 °C for 3 min and allowed to form duplex DNA substrates at room temperature for at least 30 min. Oligonucleotides containing xanthosine (X) or oxanosine (O) were prepared as previously described (*4*, *9*).

Tma Endo V Cleavage Assays. Cleavage reaction mixtures (10 μL) containing 10 mM HEPES−KOH (pH 7.4), 1 mM DTT, 2% glycerol, 5 mM $MgCl_2$ (unless otherwise specified), 10 nM oligonucleotide DNA substrate, and the indicated amount of Tma endo V protein were incubated at 65 °C for 30 min. Reactions were terminated by addition of an equal volume of GeneScan stop buffer. The reaction mixtures were then heated at 94 °C for 3 min and chilled on ice, and 3.5 μL was loaded onto a 10% denaturing polyacrylamide gel containing 7 M urea. Electrophoresis was conducted at 1500 V for 1.6 h using an ABI 377 sequencer (Applied Biosystems). Cleavage products and remaining substrates were quantified using the GeneScan analysis software version 3.0.

Gel Mobility Shift Assays. Binding reaction mixtures (20 μL) containing 100 nM fluorescently labeled oligonucleotide DNA substrates, 5 mM $CaCl_2$ or 5 mM EDTA, 20% glycerol, 10 mM HEPES−KOH (pH 7.4), 1 mM DTT, and the indicated amount of Tma endo V protein were incubated at 65 °C for 30 min. Samples were electrophoresed on a 6% native polyacrylamide gel in 1 × TB buffer supplemented with 5 mM $CaCl_2$ or EDTA. The bound and free DNA species were analyzed using a Typhoon 9400 imager (Amersham Biosciences) with the following settings: PMT at 600 V, excitation at 495 nm, and emission at 535 nm.

RESULTS

Site-Directed Mutagenesis in the Active Site of Tma Endo V. Endonuclease V is a metal-dependent enzyme. Analysis of conserved residues indicates that D43 in motif II, E89 in motif III, and D110 in motif IV are invariant in the endo V protein family (Figure 1). Large-scale sequence alignment also reveals the highly conserved nature at H214 in motif VII (Figure 1). The invariant H116 in motif IV is involved in DNA interaction rather than directly in catalysis (*6*). To probe the functional role of D43, E89, D110, and H214 in catalysis, a series of site-directed mutants were constructed. The amino acid substitutions were designed to potentially maintain metal binding (D43C, D43H, and D43E, for example) or eliminate metal binding (D43A) (Figure 1). Mutant proteins were overexpressed by induction in low phosphate medium (*2*), with the exception of E89C, which was expressed at low levels and was not pursued in subsequent studies.

Effect of Mutations on Cleavage of Substrates Harboring Deaminated Bases. We initially investigated the cleavage activity of the 15 mutants along with the wt Tma endo V as a control. Cleavage assays were performed using a fluorescently labeled (FAM) double-stranded single-inosine oligonucleotide DNA substrate (Figure 2A). Since endo V cleaves at the second phosphodiester bond one nucleotide from the 3′ side of the deaminated base, the cleavage reaction generates a 38-mer fragment, which can be visualized and quantified by GeneScan analysis on a DNA sequencer. A representative gel picture is shown in Figure 2B, and complete results of cleavage assays are summarized in Table 1. To prepare all four deaminated DNA bases including inosine, xanthosine, oxanosine, and uridine, we either

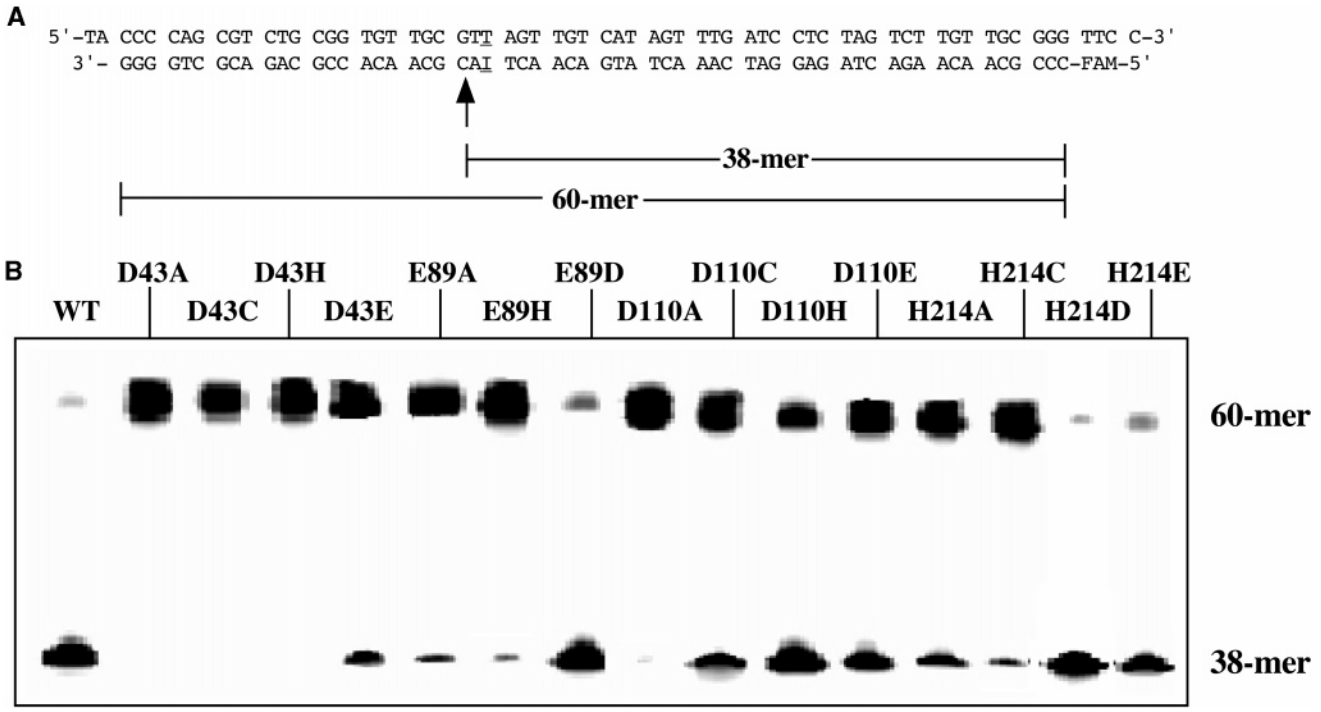

FIGURE 2: DNA cleavage assay of Tma endonuclease V. (A) Lesion-containing deoxyribooligonucleotide substrate. I = deoxyinosine. The bottom strand was 5′ labeled with FAM fluorophore. (B) Cleavage activity of wt and mutant Tma endo V on inosine-containing substrate (C/I). Cleavage reactions were performed as described in Experimental Procedures using 100 nM wt or mutant Tma endo V protein.

Table 1: Percent Cleavage of Inosine-, Xanthosine-, Oxanosine-, and Uridine-Containing DNA[a]

	inosine		xanthosine		oxanosine		uridine	
endo V	T/I	ss I	T/X	ss X	T/O	ss O	G/U	ss U
wt	100	100	100	100	100	100	100	100
D43A	0	0	3	1	0	0	0	0
D43C	0	7	10	10	0	1	2	0
D43H	0	4	2	4	0	1	1	0
D43E	31	24	34	35	5	5	1	0
E89A	24	9	31	30	3	3	6	0
E89H	10	4	9	16	0	3	1	0
E89D	95	100	99	100	12	19	6	5
D110A	3	2	2	2	1	1	2	7
D110C	53	82	55	53	3	7	2	6
D110H	60	10	59	77	5	6	1	4
D110E	40	57	83	72	10	16	6	1
H214A	40	80	48	64	5	9	4	0
H214C	17	34	29	34	3	4	2	1
H214D	102	94	95	96	78	56	61	31
H214E	89	100	99	101	13	16	7	5

[a] The reactions were performed as described in Experimental Procedures with 100 nM endo V, 10 nM substrate, and 5 mM $MgCl_2$.

purchased or synthesized single lesion-containing oligonucleotide DNA substrates in house as described in Experimental Procedures.

Of the four residues studied, D43 appears to be the least mutable site, as evidenced by no more than 10% cleavage using any of the D43 mutants on the panel of eight double-stranded and single-stranded substrates (Table 1). The conserved substitution in the D43E mutant retained ~30% cleavage activity on inosine and xanthosine substrates, but little cleavage on oxanosine or uridine was observed (Table 1). E89A showed ~20−30% inosine and xanthosine cleavage and little oxanosine and uridine cleavage, consistent with a previous study on the inosine substrate (*8*). E89H was not as active as E89A, indicating that the imidazole side chain cannot substitute for the negatively charged carboxyl group in E89. E89D had cleavage activity similar to that of the wt enzyme on inosine and xanthosine substrates, but the cleavage activity on oxanosine and uridine substrates was substantially reduced (Table 1).

Elimination of the carboxyl group in D110 by mutation to Ala severely crippled the enzyme, as the D110A mutant exhibited little cleavage activity on all substrates (Table 1). D110C, D110H, and the conservative change D110E still retained more than 40% cleavage activity on inosine and xanthosine substrates, while the cleavage activity on oxanosine and uridine substrates was reduced to less than 10% (Table 1). These results suggest that D110 is more tolerant of side chain substitutions that could participate in metal binding. Notably, the equivalent position in *Pyrococcus furiosus* endo V is Glu instead of Asp (Figure 1).

H214 is a residue most tolerant of mutation without impacting activity (Table 1). The least active H214C mutant still showed about 20−30% inosine and xanthosine cleavage activity, while H214A was about 50% active on double-stranded inosine and xanthosine substrates. Substitution of an imidazole side chain by the carboxyl group, as seen in H214D and H214E, had little effect on inosine and xanthosine cleavage. H214D also retained significant oxanosine and uridine cleavage activity, making it the most similar mutant to the wt enzyme based on deaminated base cleavage activity (Table 1). These data were in keeping with the exchangeability between His and Asp in this position that is seen in endo V family proteins (Figure 1).

The wt Tma endo V demonstrates single-turnover kinetics on inosine substrate as a result of tight binding to the nicked inosine-containing DNA (*2*). Given the similarity between the wt enzyme and H214D, we were curious to determine if the substitution would alter kinetic behavior. We therefore

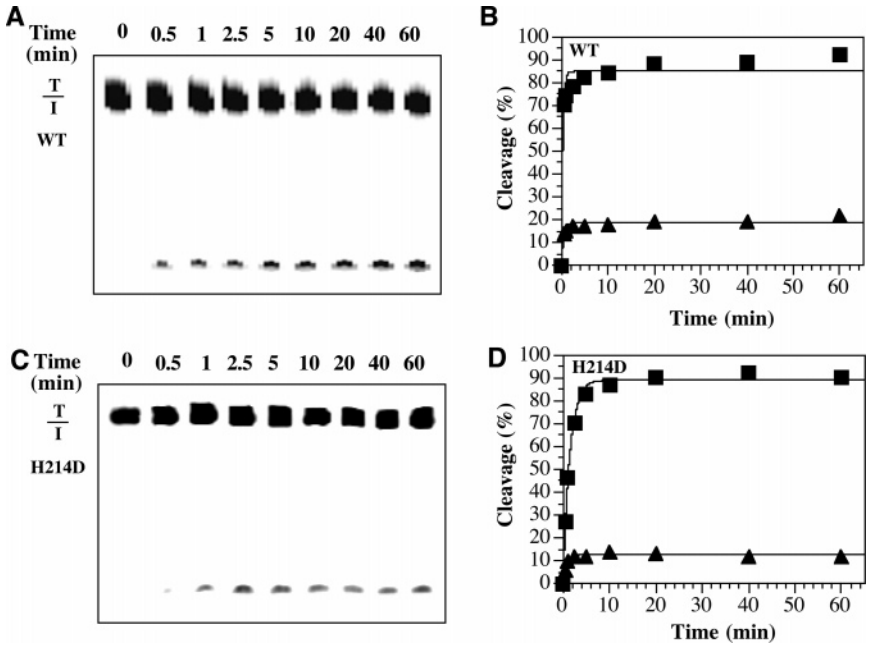

FIGURE 3: Time course analysis of T/I cleavage by wt Tma endo V and the H214D mutant. Cleavage reactions were performed as described in Experimental Procedures except that the E:S ratio was 1:10 (triangle) and 10:1 (square), respectively. Reactions were stopped on ice at indicated time points, followed by the addition of an equal volume of GeneScan stop buffer. (A) GeneScan gel analysis of T/I cleavage by wt endo V (E:S = 1:10). (B) Plots of T/I cleavage by wt endo V. (C) GeneScan gel analysis of T/I cleavage by the H214D mutant (E:S = 1:10). (D) Plot of T/I cleavage by the H214D mutant.

conducted a time-course analysis using the double-stranded inosine substrate. When the enzyme was in excess ([enzyme]:[substrate] = 10:1), both the wt enzyme and H214D showed close to complete turnover of the inosine substrate (Figure 3). When the substrate was in excess ([enzyme]:[substrate] = 1:10), H214D exhibited a similar single-turnover kinetics as seen in the wt enzyme (Figure 3). These results indicate that alteration of H214 to Asp, which is found in eukaryotic endo V homologues, may maintain the same kinetic property on inosine cleavage (Figures 1 and 3).

Effects of Mutation on Binding Affinity to Inosine-Containing Substrate. To understand the effects of these mutants on binding, we conducted gel mobility shift assays using the double-stranded inosine-containing substrate. Consistent with a previous study (*8*), D43A, D43C, and D43H showed greater binding to the inosine substrate than the wt enzyme in the absence of metal cofactor (Figure 4). D43E, in a manner similar to the wt enzyme, maintained weak binding in the absence of metal cofactor. As stated previously (*8*), these results suggest that elimination of the negative charge at D43 may reduce repulsion with the negatively charged DNA backbone. The same notion can be applied to E89 in which the E89D mutant showed a similarly weak binding in the absence of metal cofactor (Figure 4).

D110E behaved differently from the D43E and E89D mutants as it exhibited tighter binding than the wt enzyme. Unlike D110A and D110H, D110C did not show a strong binding in the absence of metal cofactor (Figure 4). These results underscore the difference between D43 and D110 as to metal or DNA binding. Mutations at H214 reduced the binding affinity in the absence of metal cofactor, in particular when it was substituted by the negatively charged Asp or Glu (Figure 4). Addition of the catalytically inactive metal cofactor Ca^{2+} brought the binding affinity of D43E, E89D, and H214D/E to a level more comparable to the mutants of the same site, consistent with the notion that a metal ion may bridge the negatively charged DNA backbone and the carboxyl group.

Effects of Mn^{2+} on T/I Cleavage. Mn^{2+} can sometimes rescue the activity of nuclease mutants (*10*−*13*). To test the effects of substituting Mn^{2+} for Mg^{2+} on inosine cleavage, we examined the cleavage activity on the double-stranded inosine substrate. Among the 15 mutants tested, 7 showed enhanced cleavage activity in the presence of Mn^{2+} (Figure 5). At the D43 site, D43E was the sole mutant with enhanced cleavage activity. Although the cleavage activity of E89A and E89H was low in the presence of Mg^{2+}, both cleavage activities were significantly enhanced with Mn^{2+} as the metal cofactor. D110A, D110C, and D110H showed different degrees of Mn^{2+} rescue (Figure 5). The most significant rescuing effect was observed with D110A, in which cleavage of the inosine substrate reached ~40%. Of the H214 mutants, only H214A was more active with Mn^{2+} than with Mg^{2+} (Figure 5). The mechanism underlying the observed Mn^{2+} effects is not obvious. It may be related to how well Mn^{2+} can be coordinated by the mutants.

3′-Exonuclease Activity of Endo V Mutants. Previously, we reported 3′-exonuclease activity from endo V in the presence of Mn^{2+} (*6*). In the course of investigating Mn^{2+} effects as described above, we also observed a laddered banding pattern below the specific cleavage product, indicative of 3′-exonuclease activity (Figure 6). This activity could not have come from contaminating *E. coli* enzymes since the similarly purified active site inactive mutant D43A and other mutants such as G136V did not show such activity (ref *6* and data not shown). In the presence of Mn^{2+}, 3′-exonuclease activity was pronounced in wt endo V and mutant enzymes E89D, D110C, H214C, H214E, and H214D, while reduced activity was detected in D110A, D110H, and D110E (Figure 6). These results indicate that some mutations

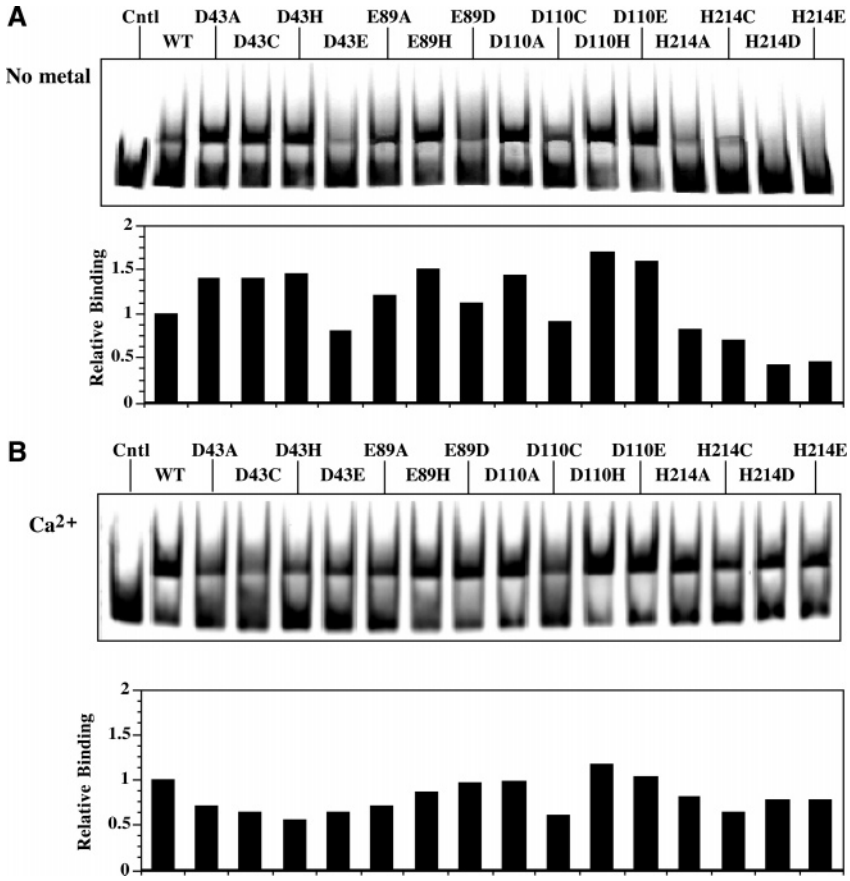

FIGURE 4: Binding analysis of Tma endo V mutants on double-stranded inosine-containing DNA substrate. Gel mobility shift analysis of binding of Tma endo V to double-stranded inosine-containing substrate (T/I) without metal ion (A) and with 5 mM $CaCl_2$ (B). Gel mobility shift assays were performed as described in Experimental Procedures using 100 nM wt or mutant Tma endo V protein and 100 nM T/I substrate.

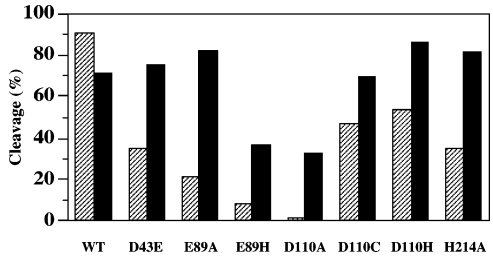

FIGURE 5: Effects of Mn^{2+} on cleavage of T/I substrate by wt and mutant Tma endo V. Cleavage reactions were performed as described in Experimental Procedures using 100 nM wt or mutant Tma endo V protein and 5 mM $MgCl_2$ (hatched bars) or $MnCl_2$ (solid bars).

have caused a reduction in the 3′-exonuclease processivity, resulting in the unique laddering effect (*6*). The 3′-exonuclease in D43E, E89A, E89H, and H214A appeared to be substantially reduced. Co^{2+}, another metal ion that in part supports endo V activity (*4*, *14*), only weakly supported 3′-exonulcease activity in the H214C and H214D mutants (Figure 6).

Effects of Ca^{2+} on Mn^{2+}-Mediated Cleavage. Although Ca^{2+} does not support the cleavage activity, it enables endo V to bind to DNA (*4*, *8*). Previous studies demonstrated that Ca^{2+} can also enhance the Mn^{2+}-mediated cleavage activity of *Eco*RV restriction endonuclease, which was taken as an indication of a two-metal catalytic mechanism (*15*). This model has been supported by subsequent structural studies (*16*, *17*). To assess the potential Ca^{2+} effects on Mn^{2+}-mediated DNA cleavage, we supplemented different concentrations of Ca^{2+} in the inosine cleavage reactions in the presence of Mn^{2+}. With increasing Ca^{2+} concentrations, we observed a decrease in the remaining substrate band and an increase in the specific cleavage band (38-mer) for E89D, D110C, H214D, and the wt enzyme (Figure 7). Apparently, as with *Eco*RV and *Taq*I endonuclease (*15*, *18*), Ca^{2+} stimulates the Mn^{2+}-mediated catalytic activity of endo V.

Effects of Mn^{2+} on Mg^{2+}-Mediated Cleavage. On the basis of the stimulatory effect Ca^{2+} had on Mn^{2+}-mediated cleavage, we then investigated the effects of Mn^{2+} on Mg^{2+}-mediated cleavage. With increasing Mn^{2+} concentrations, full-length substrate cleavage was enhanced, indicating that Mn^{2+} stimulated Mg^{2+}-mediated wt endo V cleavage (Figure 8). Interestingly, the reaction was inhibited by Mn^{2+} concentrations higher than 2.5 mM as evidenced by the reappearance of uncleaved substrate (Figure 8A). The depletion of the remaining substrate band corresponded with increased intensities in the bands below the specific cleavage product. These results suggest that Mn^{2+} stimulated nonspecific cleavage which could be the result of endonuclease and/or exonuclease action as previously reported (*2*, *6*). E89D and D110C showed increased nonspecific cleavage with increasing Mn^{2+} concentrations. A gradual and small decrease in the remaining substrate was observed with increasing Mn^{2+} concentration up to 2.5 mM in H214D. A common feature demonstrated by the wt endo V and the three mutants was that increased Mn^{2+} concentration was accompanied by increased laddering effect below the specific cleavage band,

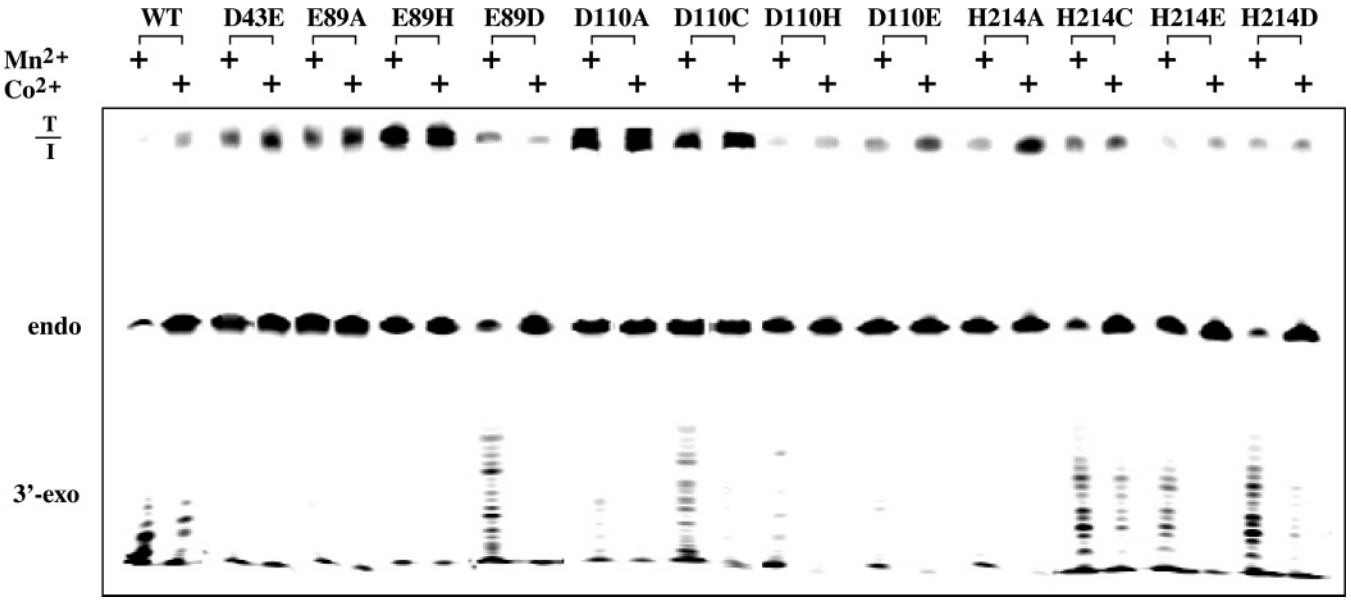

FIGURE 6: Cleavage of T/I substrate by wt and mutant Tma endo V in the presence of Mn^{2+} or Co^{2+}. Cleavage reactions were performed as described in Experimental Procedures using 100 nM wt or mutant Tma endo V protein and 5 mM $MnCl_2$ or $CoCl_2$.

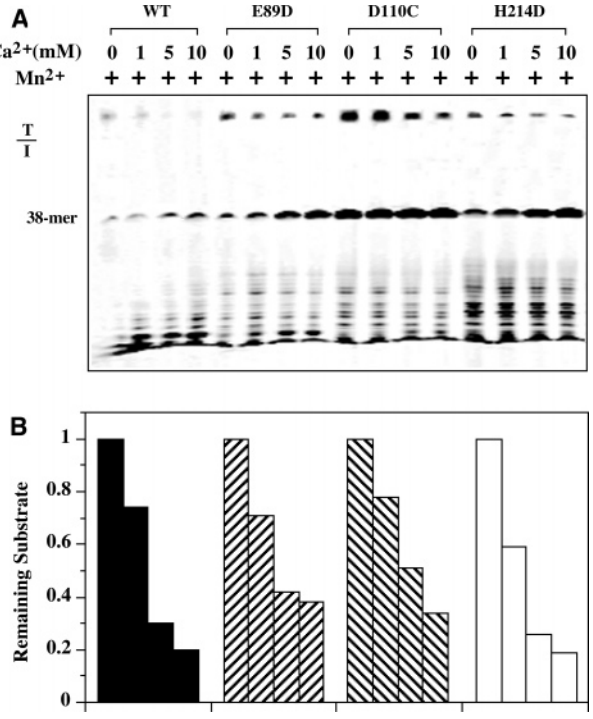

FIGURE 7: Cleavage of T/I substrate by wt and mutant Tma endo V in the presence of Mn^{2+} and Ca^{2+}. (A) Cleavage reactions were performed as described in Experimental Procedures using 100 nM wt or mutant Tma endo V protein, 5 mM $MnCl_2$, and indicated concentrations of $CaCl_2$. (B) Quantitation of uncleaved full-length substrate by GeneScreen gel analysis.

suggesting reduced processivity of the 3′-exonuclease activity from endo V (*6*).

DISCUSSION

Endonuclease V is a highly conserved metal-dependent DNA repair enzyme. Based on extensive sequence alignment, this work probes the active site organization of endonuclease V by comprehensively analyzing a series of site-directed mutant Tma endo V proteins. Effects of active site mutations were assessed for their impact on DNA binding and cleavage. In this study, different combinations of metal ions were used to gain insight on metal binding in the active site and catalytic mechanism, which led to the proposal of a catalytic and regulatory two-metal model.

Cleavage, Binding, and Active Site. The effects on DNA cleavage were examined using substrates containing four types of deaminated bases. Overall, oxanosine and uridine cleavage activity was notably sensitive to perturbation by mutagenesis. Previously, we found that many endo V mutants were inactive on substrates containing oxanosine and uridine and suggested a hypothetical deaminated base recognition model to explain these observations (*6*). It is likely that the lack of favorable interactions with oxanosine and uridine makes the oxanosine and uridine cleavage more sensitive to subtle changes in the active site.

Of the residues studied here, D43 is the least tolerant to mutation, as evidenced by loss of DNA cleavage in D43A, D43C, and D43H. The cleavage data, combined with the binding analysis, strongly suggest that D43 is an important residue involved in metal binding at the active site. These analyses were consistent with the invariant nature observed in endo V family proteins (Figure 1).

The conserved Asp substitution was well tolerated at E89 for inosine and xanthosine cleavage (Table 1). However, the negatively charged carboxyl group does not seem to be essential for catalysis as E89A still retains significant inosine and xanthosine cleavage activity. Both E89A and E89H were stimulated by substituting Mn^{2+} for Mg^{2+} (Figure 5), suggesting a potential supportive role of E89 in metal binding.

D110 is another putative metal binding residue identified by previous alanine scanning mutagenesis (*8*). Although Ala substitution essentially inactivates the enzyme in the presence of Mg^{2+} (ref *8* and Table 1), other residues that potentially can serve as metal ligand such as Cys or His rescued the inosine and xanthosine cleavage activity to a level that is comparable to the conserved D110E change, which maintains the carboxyl group (Table 1). The mutability at D110 was further demonstrated by the stimulatory effects observed in

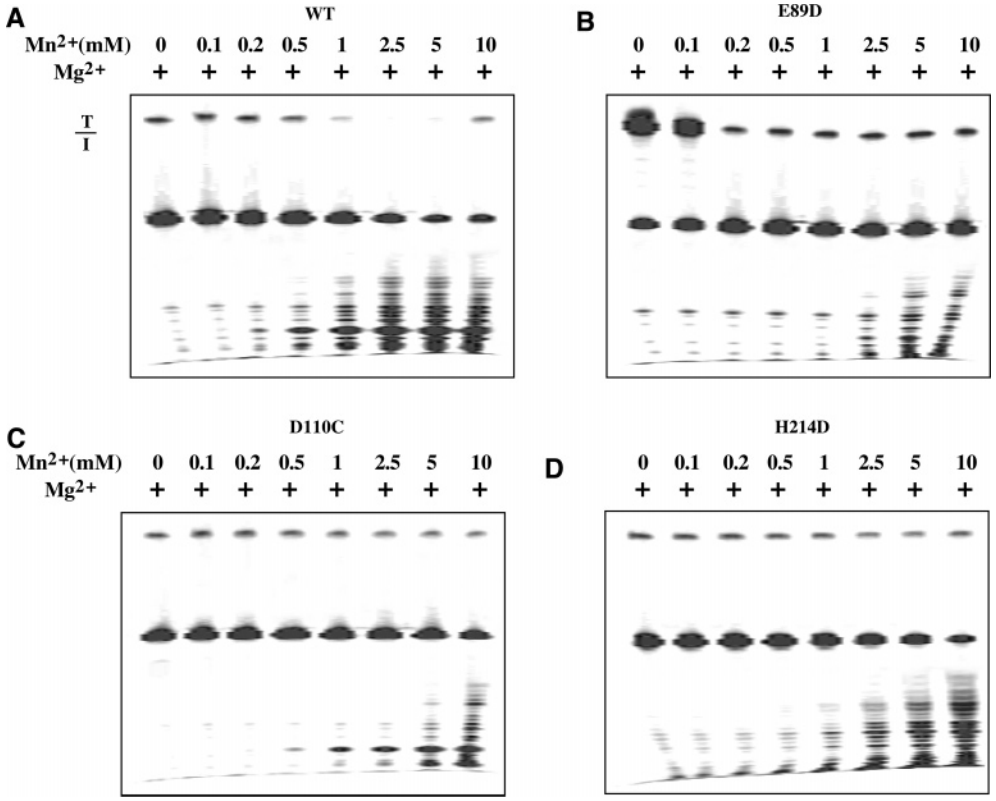

FIGURE 8: Influence of Mn^{2+} on $MgCl_2$-mediated cleavage of T/I substrate. Cleavage reactions were performed as described in Experimental Procedures using 100 nM wt or mutant Tma endo V protein, 5 mM $MgCl_2$, and indicated concentrations of $MnCl_2$. Panels: (A) wt endo V; (B) E89D; (C) D110C; (D) H214D.

D110C, D110H, and D110A when Mn^{2+} was substituted for Mg^{2+} (Figure 5).

H214 is the residue most tolerant to mutagenesis of the four amino acid positions studied, as evidenced by the fact that none of the mutations completely inactivated the enzyme (Table 1). Introduction of negatively charged carboxyl groups to H214 (H214D and H214E) appeared to reduce the binding affinity of the protein to DNA (Figure 4). These results implicate that likelihood of this site as a metal binding ligand to interact with the negatively charged DNA backbone in the active site, in a way similar to other carboxyl-containing sites. H214D, which is a conserved change found in mammalian endo Vs (Figure 1), retains significant cleavage activity toward all four deaminated bases (Table 1), indicating that His and Asp are interchangeable at this site. H214D also resembles the wt enzyme in single-turnover cleavage kinetics (Figure 3), indicating that endo V family proteins with Asp at this site can serve as a sensor/recruiter for the downstream repair process as previously proposed for the wt Tma endo V enzyme (*2*). Indeed, *E. coli* and *Salmonella* endo V, which also have an Asp at the position equivalent to H214, demonstrate similar kinetic behavior (*4*, *19*).

Interestingly, recent analysis of the sequence profile coupled with secondary-structure prediction placed endo V, the PIWI domain of Argonaute 2 (Ago-2, slicer in RNA interference), RNase H, and UvrC into a structurally homologous group (*20*). Combined with previously identified members, this nuclease superfamily expands to including retroviral integrase, RuvC and exonuclease III, and DNase I (*21*, *22*). Spatially speaking, D43, E89, D110, and H214 in Tma endo V bear some similarity to D10, E48, D70, and D134 in RNase H (*23*, *24*), indicating a potential evolutionary conservation of metal binding ligands in the superfamily.

A Catalytic and Regulatory Two-Metal Model. Previous studies on the effects of Mn^{2+} on cleavage of oxanosine and inosine substrates showed that Mn^{2+} stimulates nonspecific cleavage at low concentrations while being inhibitory at high concentrations (*5*). The underlying biochemical mechanism for this observation remains unclear. To explore the possibility that two metal ions may be involved in regulation of enzymatic activity, we conducted a series of dual metal assays. Addition of increasing concentrations of Ca^{2+} (which does not support catalysis) to the Mn^{2+}-mediated cleavage reaction resulted in stimulation of cleavage (Figure 7). This Ca^{2+}-mediated stimulation may be the result of occupation of the regulatory site by Ca^{2+}. Interestingly, cleavage activity of *Eco*RV on the cognate site has been shown to be enhanced by supplementing Ca^{2+} to the Mn^{2+}-mediated reaction (*15*). Similarly, *Eco*RV activity on the noncognate substrate is initially enhanced by $Ca^{2+}-Mn^{2+}$ combinations at low Ca^{2+} concentrations and then inhibited at higher Ca^{2+} levels (*15*). The Ca^{2+} effects were consistent with the observation of two metal ions in the active site of *Eco*RV (*16*). Analyses of metal dependence and crystal structure of RNase H and FLAP endonuclease also led to a two-metal model for regulation of nuclease activity (*24*−*26*).

On the basis of data obtained from this and previous studies (*5*), we propose a catalytic and regulatory two-metal-ion model for endo V. This model posits that endo V possesses two metal binding sites (M1 and M2) (Figure 9). Occupation of the M1 site by a catalytic metal such as Mg^{2+} or Mn^{2+} is required for catalysis. Occupation of the M1 site by Ca^{2+} yields an inactive endo $V-DNA-Ca^{2+}$ ternary complex. Therefore, the M1 site is a catalytic metal binding

FIGURE 9: Catalytic and regulatory two-metal model for endonuclease V. The two metal binding sites are labeled as M1 and M2. M1 is a high-affinity metal binding site. Coordination of a catalytically active metal ion triggers DNA cleavage. M2 is a low-affinity metal binding site. Occupation of the M2 site modulates the DNA cleavage activities.

site that has a relatively high affinity for metal ions. Occupation of the M2 site is not essential for catalysis, but it can regulate the specific and nonspecific activity catalyzed by the metal ion located in the M1 site (Figure 9). Depending on metal species that occupy the M1 and M2 sites, the endonuclease activity and the processivity of the 3′-exonuclease activity are altered differently.

The M1 site may coordinate Mg^{2+}, Mn^{2+}, Ca^{2+}, and other divalent metal ions. Previous metal dependence analysis indicates that very low Mg^{2+} concentration is sufficient to support complete cleavage activity (*6*), while higher Mn^{2+} concentration is required to support cleavage (*5*). These data suggest that the M1 site may possess high affinity for Mg^{2+}.

Analysis of Mg^{2+} dependence did not indicate any alteration in specific or nonspecific cleavage due to Mg^{2+} concentration (ref *6* and data not shown). These results can be explained by either lack of affinity for Mg^{2+} at the M2 site or binding of a second Mg^{2+} that does not influence the catalytic function of the Mg^{2+} located at the M1 site. Mn^{2+} however, can either stimulate or inhibit cleavage (*5*). This phenomenon can be explained if Mn^{2+} initially occupies the M1 site and then occupies the M2 low-affinity site.

In the case that two different metal ions are included in the cleavage reactions, there are three scenarios. First, supplementation of Ca^{2+} to the Mg^{2+}-mediated cleavage reaction does not seem to cause any significant effect (ref *8* and data not shown). Thus, in the Mg^{2+}-mediated cleavage reaction, regardless of whether the M2 site is occupied by Mg^{2+} or Ca^{2+}, the specific cleavage remains unaltered. Second, the main effect of supplementing Ca^{2+} to Mn^{2+}-mediated cleavage is enhanced specific cleavage with increasing Ca^{2+} concentrations (Figure 7). Apparently, occupation of the M2 site by Ca^{2+} stimulates the catalytic activity mediated by the Mn^{2+} at the M1 site. Since high Ca^{2+} concentrations do not inhibit the cleavage, it is possible that the M1 site has a higher affinity for Mn^{2+} than Ca^{2+}. Otherwise, Ca^{2+} would have displaced Mn^{2+} at the M1 site at high Ca^{2+} concentrations and inhibited the cleavage reaction. Lastly, addition of Mn^{2+} to the Mg^{2+}-mediated cleavage reaction was stimulatory at low concentration and inhibitory at higher concentrations (Figure 8A), with increasing Mn^{2+} concentrations leading to reduced processivity of the 3′-exonuclease activity. Given the distinct difference between the Mn^{2+}−Mg^{2+} and the Mn^{2+}-alone results and the high affinity of the M1 site for Mg^{2+} (Figure 8 and refs *5* and *6*), it is likely that the M1 site remains occupied by Mg^{2+} while the M2 site is occupied by Mn^{2+} at high Mn^{2+} concentrations. Consequently, the predominant catalytically active form is Mg^{2+} (M1 site)−Mn^{2+} (M2 site) in which Mg^{2+} serves as the catalytic metal ion. However, the catalytic role played by Mg^{2+} at the M1 site is modulated by Mn^{2+} at the M2 site.

Overall, the affinity of the M1 site for metal ions likely follows the order of $Mg^{2+} > Mn^{2+} > Ca^{2+}$. The M2 site should have a higher affinity to Ca^{2+} than Mn^{2+} based on the modulatory effects Ca^{2+} has on Mn^{2+}-mediated cleavage (Figure 7). The Mg^{2+}− Mn^{2+} dual metal experiments indicate that the M2 site should have a higher affinity for Mn^{2+} than Mg^{2+} to allow complex modulation of DNA cleavage (Figure 8). Thus, the affinity of the M2 site for metal ions likely follows the order of $Ca^{2+} > Mn^{2+} > Mg^{2+}$. In summary, we have presented a hypothetical two-metal model to account for the complex metal effects on various DNA cleavage activities. Evidently, more structural and biochemical analyses are needed to accurately define the metal binding pocket in the metal−endo V−DNA complex.

ACKNOWLEDGMENT

We thank Drs. Francis Barany and Jianmin Huang for providing the E89C overexpression clone. We also thank Dr. James Morris for critically reading the manuscript and editorial help. Athena Klutz and Nima Aghaebrahim participated in early work.

REFERENCES

1. Yao, M., Hatahet, Z., Melamede, R. J., and Kow, Y. W. (1994) Deoxyinosine 3′ endonuclease, a novel deoxyinosine-specific endonuclease from *Escherichia coli*, *Ann. N.Y. Acad. Sci. 726*, 315−316.
2. Huang, J., Lu, J., Barany, F., and Cao, W. (2001) Multiple cleavage activities of endonuclease V from *Thermotoga maritima*: Recognition and strand nicking mechanism, *Biochemistry 40*, 8738−8748.
3. He, B., Qing, H., and Kow, Y. W. (2000) Deoxyxanthosine in DNA is repaired by *Escherichia coli* endonuclease V, *Mutat. Res. 459*, 109−114.
4. Feng, H., Klutz, A. M., and Cao, W. (2005) Active site plasticity of endonuclease V from *Salmonella typhimurium*, *Biochemistry 44*, 675−683.
5. Hitchcock, T. M., Gao, H., and Cao, W. (2004) Cleavage of deoxyoxanosine-containing oligodeoxyribonucleotides by bacterial endonuclease V, *Nucleic Acids Res. 32*, 4071−4080.
6. Feng, H., Dong, L., Klutz, A. M., Aghaebrahim, N., and Cao, W. (2005) Defining amino acid residues involved in DNA-protein interactions and revelation of 3′-exonuclease activity in endonuclease V, *Biochemistry 44*, 11486−11495.
7. Ho, S. N., Hunt, H. D., Horton, R. M., Pullen, J. K., and Pease, L. R. (1989) Site-directed mutagenesis by overlap extension using the polymease chain reaction, *Gene 77*, 51−59.
8. Huang, J., Lu, J., Barany, F., and Cao, W. (2002) Mutational analysis of endonuclease V from *Thermotoga maritima*, *Biochemistry 41*, 8342−8350.
9. Hitchcock, T. M., Dong, L., Connor, E. E., Meira, L. B., Samson, L. D., Wyatt, M. D., and Cao, W. (2004) Oxanine DNA glycosylase activity from mammalian alkyladenine glycosylase, *J. Biol. Chem. 279*, 38177−38183.
10. Cao, W., and Barany, F. (1998) Identification of TaqI endonuclease active site residues by Fe^{2+}-mediated oxidative cleavage, *J. Biol. Chem. 273*, 33002−33010.
11. Cirino, N. M., Cameron, C. E., Smith, J. S., Rausch, J. W., Roth, M. J., Benkovic, S. J., and Le Grice, S. F. (1995) Divalent cation modulation of the ribonuclease functions of human immunodeficiency virus reverse transcriptase, *Biochemistry 34*, 9936−9943.
12. Blain, S. W., and Goff, S. P. (1996) Differential effects of Moloney murine leukemia virus reverse transcriptase mutations on RNase H activity in Mg^{2+} and Mn^{2+}, *J. Biol. Chem. 271*, 1448−1454.

13. Allingham, J. S., Pribil, P. A., and Haniford, D. B. (1999) All three residues of the Tn 10 transposase DDE catalytic triad function in divalent metal ion binding, *J. Mol. Biol. 289*, 1195−1206.
14. Yao, M., Hatahet, Z., Melamede, R. J., and Kow, Y. W. (1994) Purification and characterization of a novel deoxyinosine-specific enzyme, deoxyinosine 3′ endonuclease, from *Escherichia coli*, *J. Biol. Chem. 269*, 16260−16268.
15. Vipond, I. B., Baldwin, G. S., and Halford, S. E. (1995) Divalent metal ions at the active sites of the *Eco*RV and *Eco*RI restriction endonucleases, *Biochemistry 34*, 697−704.
16. Kostrewa, D., and Winkler, F. K. (1995) Mg^{2+} binding to the active site of *Eco*RV endonuclease: A crystallographic study of complexes with substrate and product DNA at 2 Å resolution, *Biochemistry 34*, 683−696.
17. Horton, N. C., and Perona, J. J. (2004) DNA cleavage by *Eco*RV endonuclease: Two metal ions in three metal ion binding sites, *Biochemistry 43*, 6841−6857.
18. Cao, W., and Lu, J. (2001) Exploring the catalytic center of TaqI endonuclease: Rescuing catalytic activity by double mutations and Mn(2+), *Biochim. Biophys. Acta 1546*, 253−260.
19. Yao, M., and Kow, Y. W. (1995) Interaction of deoxyinosine 3′-endonuclease from *Escherichia coli* with DNA containing deoxyinosine, *J. Biol. Chem.270*, 28609−28616.
20. Rand, T. A., Ginalski, K., Grishin, N. V., and Wang, X. (2004) Biochemical identification of Argonaute 2 as the sole protein required for RNA-induced silencing complex activity, *Proc. Natl. Acad. Sci. U.S.A. 101*, 14385−14389.
21. Yang, W., and Steitz, T. A. (1995) Recombining the structures of HIV integrase, RuvC and RNase H, *Structure 3*, 131−134.
22. Mol, C. D., Kuo, C. F., Thayer, M. M., Cunningham, R. P., and Tainer, J. A. (1995) Structure and function of the multifunctional DNA-repair enzyme exonuclease III, *Nature 374*, 381−386.
23. Katayanagi, K., Okumura, M., and Morikawa, K. (1993) Crystal structure of *Escherichia coli* RNase HI in complex with Mg^{2+} at 2.8 Å resolution: Proof for a single Mg(2+)-binding site, *Proteins 17*, 337−346.
24. Goedken, E. R., and Marqusee, S. (2001) Co-crystal of *Escherichia coli* RNase HI with Mn^{2+} ions reveals two divalent metals bound in the active site, *J. Biol. Chem. 276*, 7266−7271.
25. Keck, J. L., Goedken, E. R., and Marqusee, S. (1998) Activation/attenuation model for RNase H. A one-metal mechanism with second-metal inhibition, *J. Biol. Chem. 273*, 34128−34133.
26. Zheng, L., Li, M., Shan, J., Krishnamoorthi, R., and Shen, B. (2002) Distinct roles of two Mg^{2+} binding sites in regulation of murine flap endonuclease-1 activities, *Biochemistry 41*, 10323−10331.

BI060512B